



Title	Development of Chromatin Immunoprecipitation for the Analysis of Histone Modifications in Red Macroalga <i>Neopyropia yezoensis</i> (Rhodophyta)
Author(s)	Ueda, Shinnosuke; Mizuta, Hiroyuki; Uji, Toshiki
Citation	Molecular Biotechnology, 65, 590-597 <a href="https://doi.org/10.1007/s12033-022-00562-5">https://doi.org/10.1007/s12033-022-00562-5</a>
Issue Date	2024-06-13
Doc URL	<a href="http://hdl.handle.net/2115/92645">http://hdl.handle.net/2115/92645</a>
Rights	This version of the article has been accepted for publication, after peer review (when applicable) and is subject to Springer Nature 's AM terms of use, but is not the Version of Record and does not reflect post-acceptance improvements, or any corrections. The Version of Record is available online at: <a href="http://dx.doi.org/10.1007/s12033-022-00562-5">http://dx.doi.org/10.1007/s12033-022-00562-5</a>
Type	article (author version)
File Information	FinalFile_manuscript. revised 0822.pdf



[Instructions for use](#)

1 **Development of chromatin immunoprecipitation for the analysis of**  
2 **histone modifications in red macroalga *Neopyropia yezoensis***  
3 **(Rhodophyta)**

4  
5  
6 **Abstract**

7 Epigenetic regulation by histone modification can activate or repress  
8 transcription through changes in chromatin dynamics and regulates  
9 development and the response to environmental signals in both animals and  
10 plants. Chromatin immunoprecipitation (ChIP) is an indispensable tool to  
11 identify histones with specific post-translational modifications. The lack of a  
12 ChIP technique for macroalgae has hindered understanding of the role of  
13 histone modification in the expression of genes in this organism. In this  
14 study, a ChIP method with several modifications, based on existing protocols  
15 for plant cells, has been developed for the red macroalga, *Neopyropia*  
16 *yezoensis*, that consists of a heterogeneous alternation of macroscopic leaf-  
17 like gametophytes and microscopic filamentous sporophytes. ChIP method  
18 coupled with qPCR enables the identification of a histone mark in  
19 generation-specific genes from *N. yezoensis*. The results indicate that  
20 acetylation of histone H3 at lysine 9 in the 5' flanking and coding regions  
21 from generation-specific genes was maintained at relatively high levels, even  
22 in generation-repressed gene expression. The use of this ChIP method will

23 contribute significantly to identify epigenetic regulatory mechanisms through  
24 histone modifications that control a variety of biological processes in red  
25 macroalgae.

26

27 Key words: chromatin immunoprecipitation (ChIP); epigenetics; histone  
28 modifications; red algae; life cycle

29

### 30 **Introduction**

31 Histones are subject to an assortment of dynamic and reversible post-  
32 translational modifications (e.g., methylation, acetylation, phosphorylation,  
33 ubiquitination, etc.) that serve as a “histone code” to active or repress gene  
34 transcription (Jenuwein and Allis, 2001). For example, histone acetylation  
35 marks (especially H3 and H4 acetylation) are associated with gene activation  
36 to increase DNA access, which results from the neutralization of the basic  
37 charge in histones and the weak interaction of histones with DNA (cis effects;  
38 Allis and Jenuwein, 2016; Onufriev and Schiessel, 2019). Furthermore, the  
39 presence or absence of methylation on Lys or Arg in histones alters their  
40 association with reader proteins, which results in modifications of chromatin  
41 structure and either transcriptional repression or activation (Teperino et al.,  
42 2010). Thus, unraveling the role of the “histone code” will provide insight  
43 into many physiological processes affected by alterations in gene expression.  
44 In contrast to animals and plant, however, knowledge on the roles of post-

45 translational modifications of histone molecules in macroalgae remains  
46 limited, because of a lack of tools for histone modifications studies, except  
47 for the model brown alga *Ectocarpus* (Bourdareau et al. 2021).

48 Chromatin immunoprecipitations (ChIP) is a powerful tool to investigate  
49 interactions between DNA-binding proteins and genomic DNA. It provides  
50 important information about the role of DNA-binding proteins and putative  
51 target genes (Nelson et al., 2006). ChIP is also used to analyze the abundance  
52 and distribution of histone carrying specific covalent modifications under  
53 diverse conditions. Two methods for ChIP have been developed: X-ChIP  
54 (cross-linked chromatin followed by immunoprecipitation) and N-ChIP  
55 (native chromatin immunoprecipitation). In X-ChIP, chromatin is cross-  
56 linked using formaldehyde and then sheered by sonication or fragmented  
57 with enzymes. This is applicable to non-histone proteins that bind weakly (or  
58 indirectly) to DNA (Orlando, 2000). In N-ChIP, chromatin is isolated without  
59 cross-linking and micrococcal nuclease (MNase) is used to digest the linker  
60 DNA between the nucleosomes to maintain a native chromatin state (O'Neill  
61 and Turner, 2003; Huang et al., 2020). Although N-ChIP requires stable  
62 interactions between DNA and proteins, such as histones, it has advantages  
63 with respect to antibody specificity for analyzing histones modifications  
64 (O'Neill and Turner, 2003). Thus, it is important to develop N-ChIP methods  
65 in macroalgae to clarify their roles of histone modifications.

66 The red alga, *Pyropia/Neopyropia* (formerly *Porphyra*), belongs to the

67 Bangiales and is an important marine crop that is harvested to produce nori.  
68 The life cycle of Bangiales generally consists of a heterogeneous alternation  
69 of macroscopic leaf-like gametophytes and microscopic filamentous  
70 sporophytes. The gametophytes, which are harvested to produce food for nori  
71 or laver, form non-motile male (spermatia) and female (carpogonia) gametes  
72 on the thallus during sexual reproduction. Fertilization occurs when the  
73 female gametes are still retained on the gametophytes and successive cell  
74 divisions produce clones of the zygotes that are referred as carpospores.  
75 These develop into sporophytes, known as a *Conchocelis* phase, which was  
76 previously considered to be another species, *Conchocelis rosea* (Drew 1949;  
77 Kurogi 1953; Iwasaki 1961). The unravelling of the complete  
78 *Pyropia/Neopyropia* life cycle with an alteration of two heteromorphic  
79 generations contributes to the establishment of the mariculture system.

80 *Pyropia/Neopyropia* gametophytes usually grow in winter and  
81 produce male and female gametes at the beginning of spring. This results in  
82 the sporophytes that germinate from the zygotes growing in the summer  
83 during exposure to high temperatures. Consistent with this observation,  
84 previous studies showed differential expression of genes associated with heat  
85 stress tolerance between gametophytes and sporophytes (Luo et al., 2014; Uji  
86 et al., 2019). In addition to heat stress, generation phase-preferential genes  
87 associated with stress response and development have been characterized in  
88 *Pyropia/Neopyropia* (Uji et al., 2012; 2013; Inoue et al., 2015; Matsuda et al.,

89 2015; Uji et al., 2022).

90 To achieve the different expression pattern during generation,  
91 modifications of chromosome structure appear to be necessary for the  
92 transitions between the gametophyte and sporophyte stages of its life cycle.  
93 Indeed, the differential expression of subtypes of histones during the  
94 generation of Bangiales has been reported previously as well as the  
95 identification of putative genes encoding histone-modifying enzymes, such as  
96 histone acetyltransferase, deacetylases, histone-lysine N-methyltransferase,  
97 histone-arginine N-methyltransferase, and lysine-specific histone  
98 demethylase (Chan et al., 2012). However, there is scant evidence indicating  
99 a role for chromatin remodeling in the generation transition of red  
100 macroalgae.

101 In addition to its economic importance, fossil evidence (Butterfield,  
102 2000) and molecular phylogenetic analysis (Sutherland et al. 2011) suggest  
103 that Bangiales is an important group for elucidating the primitive  
104 mechanisms that regulate gene expression. In this study, N-ChIP method with  
105 several modifications based on existing protocols for plant cells (Saleh et al.  
106 2008; Huang et al. 2018) has been developed in *N. yezoensis*. This new ChIP  
107 method is suitable for the examination of the acetylation of histone H3 at  
108 lysine 9 (H3K9ac) in differential expression genes between the gametophyte  
109 and sporophyte stages of *N. yezoensis*. The method will increase our  
110 understanding of the role of chromatin remodeling for regulating not only life

111 cycles in the ancient lineage but also many physiological processes involved  
112 in improve productivity and quality of nori.

113

## 114 **Materials and Methods**

### 115 *Algal materials*

116 The leafy gametophytes and filamentous sporophytes of *N. yezoensis* strain  
117 TU-1 (Kuwano et al., 1996) were cultured in a medium consisting of sterile  
118 vitamin-free Provasoli's enriched seawater (PES; Provasoli, 1968) under a 10  
119 h light/14 h dark photoperiod with cool-white, fluorescent lamps at a light  
120 intensity of 40  $\mu\text{mol photons m}^{-2} \text{s}^{-1}$ .

121

### 122 *Chromatin extraction and shearing*

123 For chromatin extraction, 0.1 g (FW) of gametophytes or sporophytes were  
124 ground in liquid nitrogen with a pestle and mortar. The homogenates were  
125 mixed with 50 mL of nuclei isolation buffer [0.25 M sucrose, 15 mM 0.1 M  
126 PIPES (pH 6.8), 5 mM  $\text{MgCl}_2$ , 60 mM KCl, 15 mM NaCl, 1 mM  $\text{CaCl}_2$ ,  
127 0.9% (w/v) Triton X-100] and kept on ice for 10 min, followed by filtering  
128 through a nylon mesh (10  $\mu\text{m}$ ) to remove cell debris. The filtered  
129 homogenates were centrifuged at 6,500  $\times g$  for 20 min at 4°C and the  
130 supernatant was discarded for the isolation of nuclei. The nuclei pellets were  
131 repeatedly washed with 1 mL of nuclei isolation buffer and then with 1 mL of  
132 TE buffer, and centrifuged at 6,500  $\times g$  for 20 min at 4°C. The supernatant

133 was discarded and the pellet was resuspended in 500  $\mu$ L of micrococcal  
134 nuclease buffer [50 mM Tris-HCl (pH 7.9), 5 mM CaCl<sub>2</sub>] by gently pipetting  
135 up and down. The suspension was mixed with 0.5  $\mu$ L of micrococcal  
136 nuclease (MNase, New England Biolabs), 5  $\mu$ L of 10 mg/ml BSA, and 5  $\mu$ L  
137 of Protease Inhibitor Cocktail Set V (EDTA-free; FUJIFILM Wako Pure  
138 Chemical Corporation, Osaka, Japan) and sonicated (40 kHz, 5min, 4°C) by  
139 MCS-2 (AS ONE, Osaka, Japan), followed by incubation at 37°C for 15 min.  
140 After stopping the reaction with the addition of 2.5  $\mu$ L of 0.5 M EDTA, the  
141 sample was centrifuged at 20,000  $\times$ g for 10 min and the supernatant was  
142 transferred to a new 1.5 ml microcentrifuge tube as soluble chromatin. A 5  
143  $\mu$ L aliquot of each sample was set aside for verifying the efficiency of  
144 chromatin shearing.

145

#### 146 *Chromatin immunoprecipitation*

147 Before immunoprecipitation, Protein G Mag Sepharose beads (Cytiva,  
148 Tokyo, Japan) were rinsed with TE buffer three times, suspended in 1 mL  
149 blocking buffer (50  $\mu$ L of 10 mg/mL sheared salmon sperm DNA  
150 (Biodynamics Laboratory Inc, Tokyo, Japan), 50  $\mu$ L of 10 mg/mL BSA (New  
151 England Biolabs), and 900  $\mu$ L of TE buffer) and gently rotated at 4°C  
152 overnight to block the beads. Blocked beads were rinsed with TE buffer and  
153 then resuspended with TE buffer equivalent to the amount of beads added.  
154 For preclearing, 500  $\mu$ L of chromatin solution was transferred to a 1.5 mL



155 tube containing 30  $\mu$ L of blocked beads, 7  $\mu$ L of Protease Inhibitor Cocktail  
156 Set V (EDTA free), and 700  $\mu$ L of TE buffer and rotated with a tube rotator  
157 at 4°C for 2h. After removing the beads using a magnetic stand, 400  $\mu$ L of  
158 pre-cleared chromatin was split into three 1.5 mL tubes (antibody of interest,  
159 negative and positive controls) containing 400  $\mu$ L of TE buffer. Pre-cleared  
160 chromatin (10  $\mu$ L) was kept at 4°C to serve as an ‘input’ DNA control. For  
161 immunoprecipitation, 2  $\mu$ L (2  $\mu$ g) of monoclonal antibody (anti-H3K9ac) and  
162 2  $\mu$ L (2  $\mu$ g) of monoclonal H3 antibody (positive control) were added to each  
163 of the three tubes containing pre-cleared chromatin. The other tube without  
164 any antibody served as a negative control. All tubes were incubated with  
165 gentle rotation overnight at 4 °C. After incubation, 25  $\mu$ L of newly blocked  
166 beads were added to each tube, which were incubated with gentle rotation at  
167 4°C for 2 h. After removing the supernatant, the beads were washed three  
168 times sequentially with low salt wash buffer [75 mM NaCl, 1 mM EDTA, 10  
169 mM Tris-HCl (pH 8.1), 0.1% SDS, 1% Triton X-100]. For eluting the DNA,  
170 200 or 190  $\mu$ L of ChIP elution buffer (1% SDS, 100 mM NaHCO<sub>3</sub>)  
171 containing 1.0  $\mu$ L of RNase A (100 mg/ml) (NIPPON GENE, Tokyo, Japan).  
172 was added to each tube containing beads or chromatin solution for input,  
173 respectively, and incubated at 68°C for 2 h. The antibodies were purchased  
174 from Monoclonal Antibody Research Institute, Inc. (Nagano, Japan).  
175  
176 *ChIP-qPCR analysis*

177 For ChIP-qPCR experiments, the eluted DNA was purified using a QIAquick  
178 PCR Purification Kit (Qiagen, Hilden, Germany) following the  
179 manufacturer's instructions. For each reaction, 1.0 µl of DNA was used as a  
180 template in a 20 µL reaction volume containing KOD SYBR® qPCR Mix  
181 (TOYOBO, Osaka, Japan). ChIP-qPCR was performed based on the  
182 manufacturer's instructions using a LightCycler® 480 System (Roche  
183 Diagnostics, Basel, Switzerland) under the following conditions: 2 min at  
184 98°C followed by 45 cycles of 10 s at 98°C, 10 s at 55°C, and 30 s at 68°C.  
185 ChIP-qPCR data were analyzed to determine the pull-down efficiency  
186 relative to the input. Ct values were used for performing the calculation,  
187 which consisted of evaluating the fold-difference between the experimental  
188 sample and normalized input as follows:  $\Delta Ct [\text{normalized ChIP}] = (Ct [\text{ChIP}]$   
189  $- (Ct [\text{Input}] - \text{Log}_2 (\text{Input Dilution Factor})))$ . The percentage (Input %) value  
190 for each sample was calculated as follows:  $\% \text{ Input} = 2^{(-\Delta Ct [\text{normalized}$   
191  $\text{ChIP}])} * 100$ . The "Input %" value represents the enrichment of a histone  
192 modification in a specific region. qPCR was performed in triplicate. Table S1  
193 lists the primers that were used for these analyses.

194

#### 195 *Transcriptional analysis*

196 Total RNA from gametophytes and sporophytes (Fresh weight: 0.05–0.1 g)  
197 was separately extracted using the RNeasy Plant Mini Kit (Qiagen, Hilden,  
198 Germany) in liquid nitrogen with a mortar and pestle, following the

199 manufacturer's instructions. The extracted RNA was purified using a  
200 TURBO DNA-free kit (Invitrogen/Life Technologies, Carlsbad, CA) to  
201 obtain DNA-free RNA. First strand cDNA was synthesized from 0.5 µg total  
202 RNA using the PrimeScript II First Strand cDNA Synthesis Kit (TaKaRa  
203 Bio, Shiga, Japan). The cDNA was diluted 10-fold for qRT-PCR analysis.  
204 For each reaction, 1.0 µl of the diluted cDNA was used as a template in a 20  
205 µL reaction volume containing KOD SYBR® qPCR Mix. Quantitative RT-  
206 PCR was performed as per the manufacturer's instructions using a  
207 LightCycler® 480 System under the following conditions: 2 min at 98°C  
208 followed by 40 cycles of 10 s at 98°C, 10 s at 55°C and 30 s at 68°C. The  
209 mRNA levels were calculated using the  $2^{-\Delta\Delta C_t}$  method and normalized to the  
210 expression of the 18S ribosomal RNA (*18SrRNA*) gene (Uji et al., 2016).  
211 Relative expression levels were calculated as the ratio of the observed mRNA  
212 levels present in the gametophytes. The PCR reactions were performed in  
213 triplicate. Table S2 lists the primers that were used for these analyses.

214

## 215 **Results and discussion**

### 216 *Nuclei isolation from N. yezoensis*

217 To establish the ChIP procedure (Fig. 1), a ChIP-qPCR experiment targeting  
218 *18SrRNA* in *N. yezoensis* gametophytes was performed using antibodies to  
219 histone H3. Chromatin extracts from homogenates prepared from the  
220 gametophytes were filtered through a 10 µm mesh to remove large cell

221 debris. It was also an important step to wash three times with 1 mL of nuclei  
222 isolation buffer and TE buffer to remove large amounts of polysaccharides  
223 and photosynthetic pigments (e.g., phycobiliproteins), respectively (Fig. 2).  
224 The pull-down efficiency of *Ny18SrRNA* against H3 antibody (positive  
225 control) and no antibody (mock) using chromatin extracts without washing  
226 showed 0.39% and 0.20% relative to the input DNA in the gametophytes,  
227 respectively. In contrast, the pull-down efficiency of *Ny18SrRNA* against H3  
228 antibody and no antibody using chromatin extracts washed three times with  
229 buffer showed 1.78% and 0.06%, respectively. Thus, repeated washes were  
230 recommended using buffer before chromatin fragmentation.

231

### 232 *Chromatin fragmentation*

233 A suitable size distribution of DNA fragments is crucial for ChIP. Thus, the  
234 size distribution of genomic DNA was checked by gel electrophoresis after  
235 15 min of MNase digestion. Large amounts of chromatin fragments of  
236 suitable size (100-250 bp) for further immunoprecipitation were produced by  
237 MNase treatment with sonication, which promotes nuclease digestion of  
238 samples containing polysaccharides (Fig. 3).

239

### 240 *Chromatin immunoprecipitation and validation*

241 Next, the quality of the fragmented chromatin and the pull-down efficiency  
242 of immunoprecipitation were checked to determine the enrichment of H3.

243 The pull-down efficiency of *Ny18SrRNA* against H3 antibody and no  
244 antibody without blocking beads was 4.67% and 1.52% relative to the input  
245 DNA in the gametophytes, respectively (Fig. 4). In contrast, the pull-down  
246 efficiency of *Ny18SrRNA* against H3 antibody and no antibody using  
247 blocking beads showed 1.31% and 0.06% relative to the input DNA in the  
248 gametophytes, respectively. The fold positive control relative to mock  
249 treatment with and without blocking beads was 3.07- and 21.83-fold,  
250 respectively. Finally, in this protocol, we obtained a quantity of DNA that was  
251 sufficient to conduct 50 qPCR assays.

252 To test the quality of chromatin and the efficiency of  
253 immunoprecipitation, the protocol was applied to study histone modification  
254 patterns of the generation-preferential genes in *N. yezoensis*. Based on  
255 previous studies (Uji et al., 2012; Inoue et al., 2015; Matsuda et al., 2015),  
256 two highly upregulated genes for each generation, gametophyte and  
257 sporophyte (Table 1) were selected. As illustrated in Figure 5, the transcripts  
258 of *NyBPO* and *NyKPA1* were in high abundance in sporophytes compared  
259 with gametophytes. In contrast, the expression of *NyAly* and *NyKPA2* was  
260 decreased at sporophyte stages, whereas they were overexpressed in  
261 gametophytes. As shown in Fig. 6, ChIP-qPCR exhibited higher levels of  
262 H3K9ac enrichment for both the 5' flanking and coding regions in the  
263 generation with increased gene expression, with the exception of *NyBPO*.  
264 Histone acetylation and methylation are important chromatin modifications

265 that regulate gene expression during development and the response to  
266 environmental stress in animals and plants (Loidl 2004; Vastenhouw et al.  
267 2012; Ali et al., 2022). In particular, H3K9ac is closely associated with  
268 genes exhibiting high expression levels (Zhou et al., 2010; Kurita et al.  
269 2017). In the present study, the strong correlation between the enrichment  
270 levels of H3K9ac with transcription was not observed, suggesting that other  
271 histone marks, such as histone methylation, highly regulate the  
272 transcriptional dynamics of the *N. yezoensis* life cycle. A previous study  
273 showed that the induction of *NyKPA1* transcripts occurred rapidly in the  
274 gametophytes exposed to cold stress (Uji et al. 2012). Thus, the enrichment  
275 of H3K9ac, even in generations with suppressed expression, may be  
276 necessary for the synthesis of mRNA in response to environmental stress. In  
277 a microalga *Nannochloropsis*, H3K9ac was predominantly enriched in the 5'  
278 flanking regions and the distribution was relatively sparse in the exon regions  
279 (Wei and Xu 2018). In contrast, a decrease in acetylation in exon regions was  
280 not observed in *N. yezoensis* genes in the present study.

281 A previous study showed variations in the daily expression of genes  
282 encoding MSIL-like WD40 repeat (MSIL) proteins and SET-domain proteins  
283 in the gametophytes of *N. yezoensis* (Kominami et al., 2022). MSIL proteins,  
284 which are conserved histone-binding proteins in eukaryotes, function  
285 together with histone deacetylases and methyltransferases in mammals and  
286 plants (Hennig et al. 2005). SET-domain proteins methylate lysine residues in

287 histone tails and play a fundamental role in the epigenetic regulation of gene  
288 activation and silencing in all eukaryotes (Rea et al. 2000). Thus, our ChIP  
289 method can elucidate the role of histone post-translational modifications  
290 associated with diurnal rhythm regulation in *N. yezoensis*.

291 In addition to histone modifications, epigenetic studies have revealed  
292 that DNA methylation and non-coding RNAs can alter the configuration of  
293 chromatin, which results in various chromatin states that epigenetically  
294 regulate transcriptional outputs (Ahmad et al. 2010; Skvortsova et al. 2018).  
295 To date, DNA methylation patterns during heat stress (Yu et al. 2018) and  
296 noncoding small RNAs in generations as well as under osmotic stress (He et  
297 al. 2012; Cao et al., 2019) has been identified in Bangiales. However,  
298 knowledge of epigenetic regulation of gene expression in red algae remains  
299 scant. Future studies clarifying the link among epigenetic regulators will  
300 provide insight into the role of primitive gene expression systems.

301

## 302 Conclusion

303 A ChIP method based on ChIP-qPCR, which can determine the histone  
304 modification status at different genomic regions has been developed in *N.*  
305 *yezoensis*. This method may be used for the analysis of the genome-wide  
306 distribution of specific histone modifications combined with high-throughput  
307 sequencing, such as ChIP-seq analyses. Thus, the method described here is an  
308 essential tool for elucidating the role of the “histone code” for many

309 physiological processes involved in improve productivity and quality of nori.

310

### 311 **Acknowledgments**

312 We wish to thank Drs. Katsutoshi Arai, Takafumi Fujimoto, and Toshiya

313 Nishimura (Hokkaido University, Japan) for kindly providing the

314 LightCycler 480 system.

315

### 316 **Conflict of interest**

317 The authors declare that this research was conducted in the absence of any

318 commercial or financial relationships that could be construed as a potential

319 conflict of interest.

320

### 321 **Data availability statement**

322 The data that support the findings of this study are available from the

323 corresponding author upon reasonable request.

324

### 325 **Funding**

326 This work was supported by the Grant-in-Aid for Young Scientists [grant

327 number19K15907 and 22K05779 to TU] from the Japan Society for the

328 Promotion of Science.

329

### 330 **References**



331  
332 Ahmad, A., Zhang, Y., & Cao, X.F. (2010). Decoding the epigenetic language  
333 of plant development. *Molecular Plant*, 3, 719–728.  
334  
335 Ali, S., Khan, N. & Tang, Y. (2022). Epigenetic marks for mitigating abiotic  
336 stresses in plants. *Journal of Plant Physiology*, 275, 153740.  
337  
338 Allis, C.D., & Jenuwein, T. (2016). The molecular hallmarks of epigenetic  
339 control. *Nature Reviews Genetics*, 17, 487–500.  
340  
341 Bourdareau, S., Tirichine, L., Lombard, B. Loew, D., Scornet, D., Wu, Y.,  
342 Coelho, S.M. & Cock, J. M. (2021). Histone modifications during the life cycle  
343 of the brown alga *Ectocarpus*. *Genome Biology*, 22, 12.  
344  
345 Butterfield, N. J. (2000). *Bangiomorpha pubescens* n. gen., n. sp.: implications  
346 for the evolution of sex, multicellularity, and the  
347 Mesoproterozoic/Neoproterozoic radiation of eukaryotes. *Paleobiology*, 26,  
348 386–404.  
349  
350 Cao, M., Wang, D., Kong, F., Wang, J., Xu, K. & Mao, Y. (2019). A genome-  
351 wide identification of osmotic stress-responsive microRNAs in *Pyropia*  
352 *haitanensis* (Bangiales, Rhodophyta). *Frontiers in Marine Science*, 6, 766.  
353  
354 Chan, C.X., Blouin, N.A., Zhuang, Y., Zäuner, S., Prochnik, S.E., Lindquist,  
355 E., Lin, S., Benning, C., Lohr, M., Yarish, C., Gantt, E., Grossman, A.R., Lu,  
356 S., Müller, K.W., Stiller, J., Brawley, S.H., Bhattacharya, D. (2012). *Porphyra*  
357 (Bangiophyceae) transcriptomes provide insights into red algal development  
358 and metabolism. *Journal of Phycology*, 48, 1328–1342.  
359  
360 Drew, K. (1949). Conchocelis-phase in the life history of *Porphyra umbilicalis*  
361 (L.) Kütz. *Nature*, 164, 748–749.  
362  
363 He, L., Huang, A., Shen, S., Niu, J., & Wang, G. (2012). Comparative analysis  
364 of microRNAs between sporophyte and gametophyte of *Porphyra yezoensis*.

365 *Comparative and Functional Genomics*, 912843. doi: 10.1155/2012/912843.  
366

367 Hennig, L., Bouveret, R., & Gruissem, W. (2005). MSI1-like proteins: an  
368 escort service for chromatin assembly and remodeling complexes. *Trends in*  
369 *Cell Biology*, 15, 295–302  
370

371 Huang, X.R., Pan, Q.W., Lin, Y., Gu, T.T., & Li, Y. (2020). A native chromatin  
372 immunoprecipitation (ChIP) protocol for studying histone modifications in  
373 strawberry fruits. *Plant Methods*, 16. DOI 10.1186/s13007-020-0556-z  
374

375 Inoue, A., Mashino, C., Uji, T., Saga, N., Mikami, K., & Ojima, T. (2015).  
376 Characterization of an eukaryotic PL-7 alginate lyase in the marine red alga  
377 *Pyropia yezoensis*. *Current Biotechnology*, 4, 240–248.  
378

379 Iwasaki, H. (1961). The life cycle of *Porphyra tenera* in vitro. *Biological*  
380 *Bulletin of the Marine Biological Laboratory, Woods Hole*, 121, 173–187.  
381

382 Jenuwein, T., & Allis, C.D. (2001). Translating the histone code. *Science*, 293,  
383 1074–1080.  
384

385 Kim, J.M., To, T.K., Ishida, J., Morosawa, T., Kawashima, M., Matsui, A.,  
386 Toyoda, T., Kimura, H., Shinozaki, K., & Seki, M. (2008). Alterations of lysine  
387 modifications on the histone H3 N-tail under drought stress conditions in  
388 *Arabidopsis thaliana*. *Plant & Cell Physiology*, 49, 1580–1588.  
389

390 Kominami, S., Mizuta, H., & Uji, T. (2022). Transcriptome profiling in the  
391 marine red alga *Neopyropia yezoensis* under light/dark cycle. *Marine*  
392 *Biotechnology*, 24, 393–407.  
393

394 Kurita, K., Sakamoto, T., Yagi, N., Sakamoto, Y., Ito, A., Nishino, N., Sako, K.,  
395 Yoshida, M., Kimura, H., Seki M., & Matsunaga S. (2017). Live imaging of  
396 H3K9 acetylation in plant cells. *Scientific Reports* 7, 45894.  
397

398 Kurogi, M. (1953). Studies of the life history of *Porphyra*. I. The germination

399 and development of carpospores. *Bulletin of Tohoku Regional Fisheries*  
400 *Research Laboratory*, 2, 67–103.

401

402 Kuwano, K., Aruga, Y. & Saga, N. (1996). Cryopreservation of clonal  
403 gametophytic thalli of *Porphyra* (Rhodophyta). *Plant Science*. 116, 117–124.

404

405 Loidl, P. (2004). A plant dialect of the histone language. *Trends in Plant*  
406 *Science*, 9, 84–90. DOI 10.1016/j.tplants.2003.12.007

407

408 Luo, Q., Zhu, Z., Zhu, Z., Yang, R., Qian, F., Chen, H., & Yan, X. (2014).  
409 Different responses to heat shock stress revealed heteromorphic adaptation  
410 strategy of *Pyropia haitanensis* (Bangiales, Rhodophyta). *PLoS One*, 9. doi:  
411 10.1371/journal.pone.0094354

412

413 Matsuda, R., Ozgur, R., Higashi, Y., Takechi, K., Takano, H., & Takio, S.  
414 (2015). Preferential expression of a bromoperoxidase in sporophytes of a red  
415 alga, *Pyropia yezoensis*. *Marine Biotechnology*, 17, 199–210.

416

417 Nelson, J.D., Denisenko, O., & Bomszyk, K. (2006). Protocol for the fast  
418 chromatin immunoprecipitation (ChIP) method. *Nature Protocols*, 1, 179–185.

419

420 O'Neill, L.P., & Turner, B.M. (2003). Immunoprecipitation of native chromatin:  
421 NChIP. *Methods*, 31, 76–82.

422

423 Onufriev, A.V., & Schiessel, H. (2019). The nucleosome: from structure to  
424 function through physics. *Current Opinion in Structural Biology*, 56, 119–130.

425

426 Orlando, V. (2000). Mapping chromosomal proteins in vivo by formaldehyde-  
427 crosslinked-chromatin immunoprecipitation. *Trends in Biochemical Sciences*,  
428 25, 99–104.

429

430 Provasoli, L. (1996). Media and prospects for the cultivation of marine algae.  
431 In: Watanabe A, Hattori A (eds) Culture and collections of algae, Proc U S-  
432 Japan Conf, Hakone, *Jpn Soc Plant Physiol*, Tokyo, 1968, 63–75.

433  
434 Rea, S., Eisenhaber, F., O'Carroll, D., Strahl, B.D., Sun, Z.W., Schmid, M.,  
435 Opravil, S., Mechtler, K., Ponting, C.P., Allis, C.D., & Jenuwein, T. (2000).  
436 Regulation of chromatin structure by site-specific histone H3  
437 methyltransferases. *Nature*, 406, 593–599.  
438  
439 Saleh, A., Alvarez-Venegas, R., & Avramova, Z. (2008). An efficient  
440 chromatin  
441 immunoprecipitation (ChIP) protocol for studying histone modifications in  
442 *Arabidopsis* plants. *Nature Protocols*, 3, 1018–1025.  
443  
444 Skvortsova, K., Iovino, N., & Bogdanović, O. (2018). Functions and  
445 mechanisms of epigenetic inheritance in animals. *Nature Reviews Molecular*  
446 *Cell Biology*, 19, 774–790.  
447  
448 Sutherland, J.E., Lindstrom, S.C., Nelson, W.A., Brodie, J., Lynch, M.D.J.,  
449 Hwang, M.S., Choi, H.-G., Miyata, M., Kikuchi, N., Oliveira, M.C., Farr, T.,  
450 Neefus, C., Mols-Mortensen, A., Milstein, D., & Müller, K.M. (2011). A new  
451 look at an ancient order: Generic revision of the Bangiales  
452 (Rhodophyta). *Journal of Phycology*, 47, 1131–1151.  
453  
454 Teperino, R., Schoonjans, K., & Auwerx, J. (2010). Histone methyl  
455 transferases and demethylases; Can they link metabolism and transcription?  
456 *Cell Metabolism*, 12, 321–327.  
457  
458 Uji, T., Gondaira, Y., Fukuda, S., Mizuta, H., & Saga, N. (2019).  
459 Characterization and expression profiles of small heat shock proteins in the  
460 marine red alga *Pyropia yezoensis*. *Cell Stress Chaperones*, 24, 223–233.  
461  
462 Uji, T., Hirata, R., Mikami, K., Mizuta, H., & Saga, N. (2012). Molecular  
463 characterization and expression analysis of sodium pump genes in the marine  
464 red alga *Porphyra yezoensis*. *Molecular Biology Reports*, 39, 7973–7980.  
465  
466 Uji, T., Matsuda, R., Takechi, K., Takano, H., Mizuta, H., & Takio, S. (2016).

- 467 Ethylene regulation of sexual reproduction in the marine red alga *Pyropia*  
468 *yezoensis* (Rhodophyta). *Journal of Applied Phycology*, 28, 3501–3509.
- 469
- 470 Uji, T., Mizuta, H., & Saga, N. (2013). Characterization of the sporophyte-  
471 preferential gene promoter from the red alga *Porphyra yezoensis* using  
472 transient gene expression. *Marine Biotechnology*, 15, 188–196.
- 473
- 474 Uji, T., Ueda, S., & Mizuta, H. (2022). Identification, characterization, and  
475 expression analysis of spondin-like and fasciclin-like genes in *Neopyropia*  
476 *yezoensis*, a marine red alga. *Phycology*, 2, 45–59.
- 477
- 478 Vastenhouw, N.L., & Schier, A.F. (2012). Bivalent histone modifications in  
479 early embryogenesis. *Current Opinion in Cell Biology*, 24, 374–386.
- 480
- 481 Wei, L., & Xu, J. (2018). Optimized methods of chromatin  
482 immunoprecipitation for profiling histone modifications in industrial  
483 microalgae *Nannochloropsis* spp. *Journal of Phycology*. 54, 358–367.
- 484
- 485 Yu, C., Xu, K., Wang, W. Xu, Y., Ji, D., Chen, C., & Xie, C. (2018). Detection  
486 of changes in DNA methylation patterns in *Pyropia haitanensis* under high-  
487 temperature stress using a methylation-sensitive amplified polymorphism  
488 assay. *Journal of Applied Phycology*, 30, 2091–2100.
- 489
- 490 Zhou, J., Wang, X., He, K., Charron, J.B., Elling, A.A., & Deng, X.W. (2010).  
491 Genome-wide profiling of histone H3 lysine 9 acetylation and dimethylation  
492 in *Arabidopsis* reveals correlation between multiple histone marks and gene  
493 expression. *Plant Molecular Biology*, 72, 585–595.

494

495

496

497 **Figure legends**

498 **Fig. 1.** Outline of the ChIP-qPCR protocol in *Neopyropia yezoensis*.

499

500 **Fig. 2.** Optimization of Chromatin extraction.

501 After filtering, chromatin extracts were not washed with any buffer (a),  
502 washed three times with only nuclei isolation buffer (b), or with both nuclei  
503 isolation buffer and TE buffer (c). The chromatin solution was treated with  
504 sonication and MNase. CHIP-qPCR experiment targeting the *Ny18SrRNA*  
505 gene was performed with an antibody specific to histone H3. Relative  
506 amounts of the PCR products were calculated and normalized with respect to  
507 the input chromatin. The results are presented as % Input (IP). Mock  
508 indicates the signals from the no antibody controls. The data are presented as  
509 means  $\pm$  standard deviations ( $n = 3$ ).

510

511 **Fig. 3.** Optimization of Chromatin shearing conditions.

512 After chromatin extraction, chromatin extracts were repeatedly washed three  
513 times with nuclei isolation buffer and then with TE buffer. For shearing, the  
514 chromatin solution pretreated without or with sonication was incubated with  
515 MNase at 37°C for 15 min. M: DNA marker.

516

517 **Fig. 4.** Optimization of Chromatin immunoprecipitation.

518 After chromatin extraction, chromatin extracts were repeatedly washed three  
519 times with nuclei isolation buffer and then with TE buffer. Then, the  
520 chromatin solution was treated with sonication and MNase. The CHIP-qPCR  
521 experiment targeted the *Ny18SrRNA* gene with an antibody specific to

522 histone H3, without blocking beads (a) or with blocking beads (b).

523

524 **Fig. 5.** Relative expression levels of genera genes from *Neopyropia yezoensis*

525 in gametophytes and sporophytes. RNA samples were prepared from

526 gametophytes (GA) and sporophytes (SP), and expression levels were

527 determined using the *Ny18SrRNA* gene for normalization. Relative

528 expression levels were calculated as the ratio of the observed mRNA level

529 present in the gametophytes. The data are presented as means  $\pm$  standard

530 deviations ( $n = 3$ ).

531

532 **Fig.6.** ChIP-qPCR analysis of generation-preferential genes in *Neopyropia*

533 *yezoensis*.

534 (a) Location of amplicons used in the ChIP-qPCR analysis. The boxed

535 regions indicate part of the coding sequence. The amplified sequences are

536 indicated by bars.

537 (b) The pull-down efficiencies of H3K9ac by ChIP-qPCR analysis

538 Chromatin was isolated from gametophytes (GA) and sporophytes (SP) and

539 ChIP-qPCR was targeted to *NyBPO*, *NyKPA1*, *NyAly* and *NyKPA2* using an

540 antibody specific to histone H3K9ac. Chromatin extracts were repeatedly

541 washed three times with nuclei isolation buffer and then with TE buffer.

542 Then, the chromatin solution was treated with sonication and MNase. The

543 relative amounts of PCR products were calculated and normalized with

544 respect to the input chromatin. The results are represented as % Input (IP).  
545 Mock indicates the signals from the no antibody controls. The data are  
546 presented as means  $\pm$  standard deviations ( $n = 3$ ).



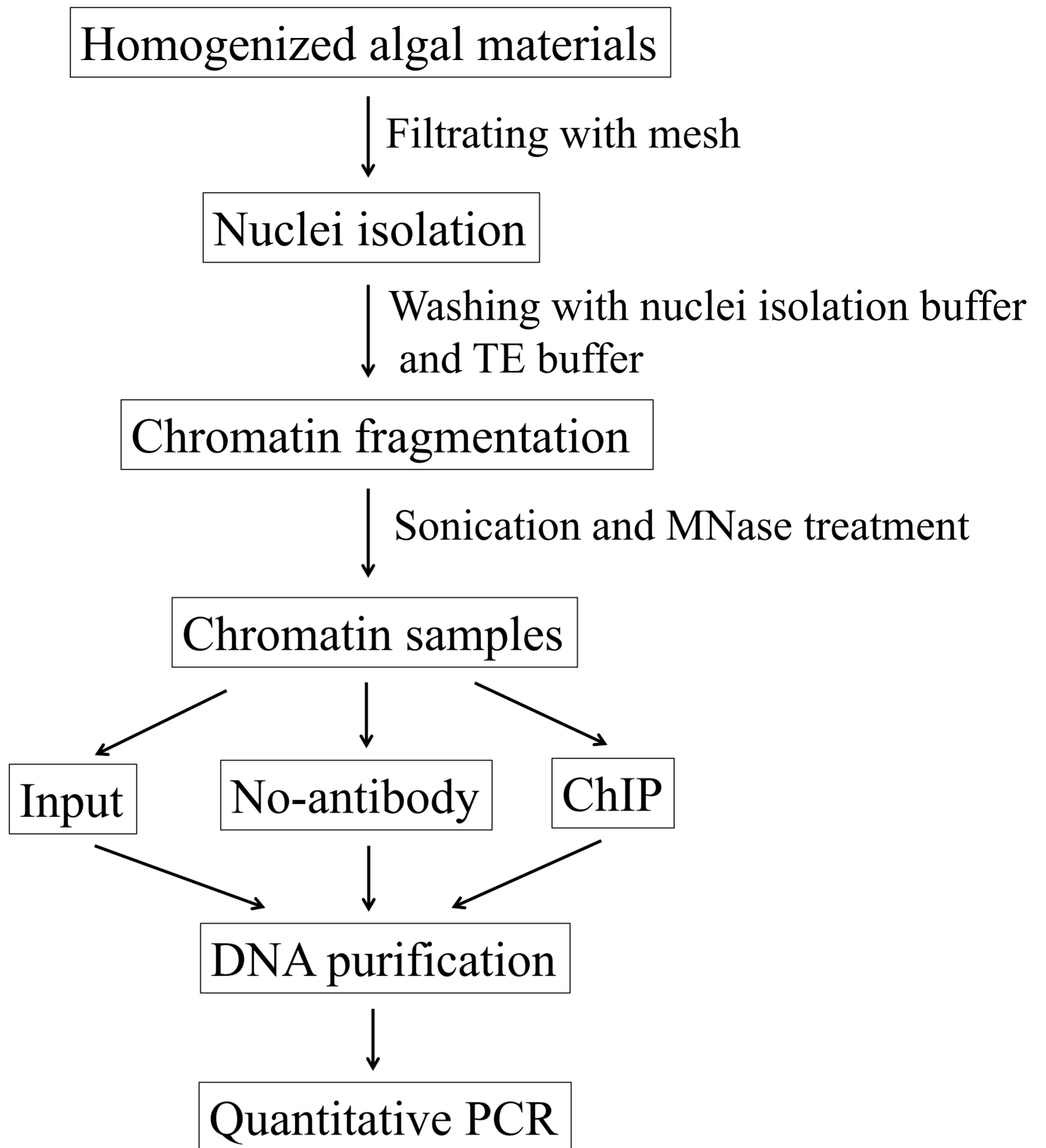


Fig.1

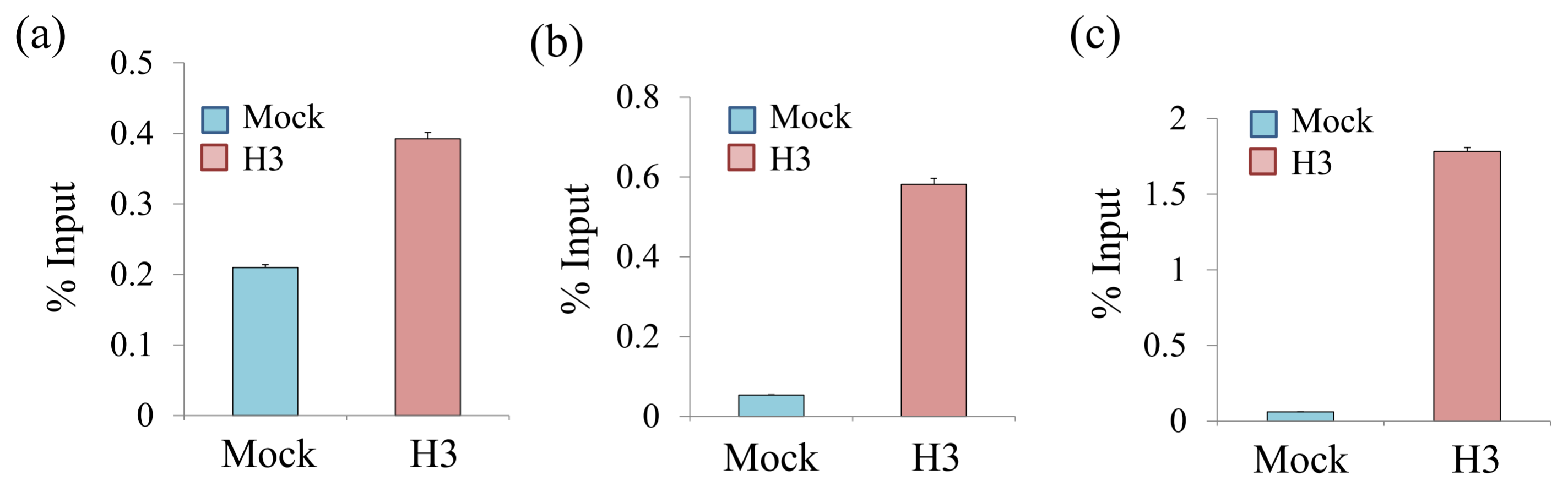


Fig.2

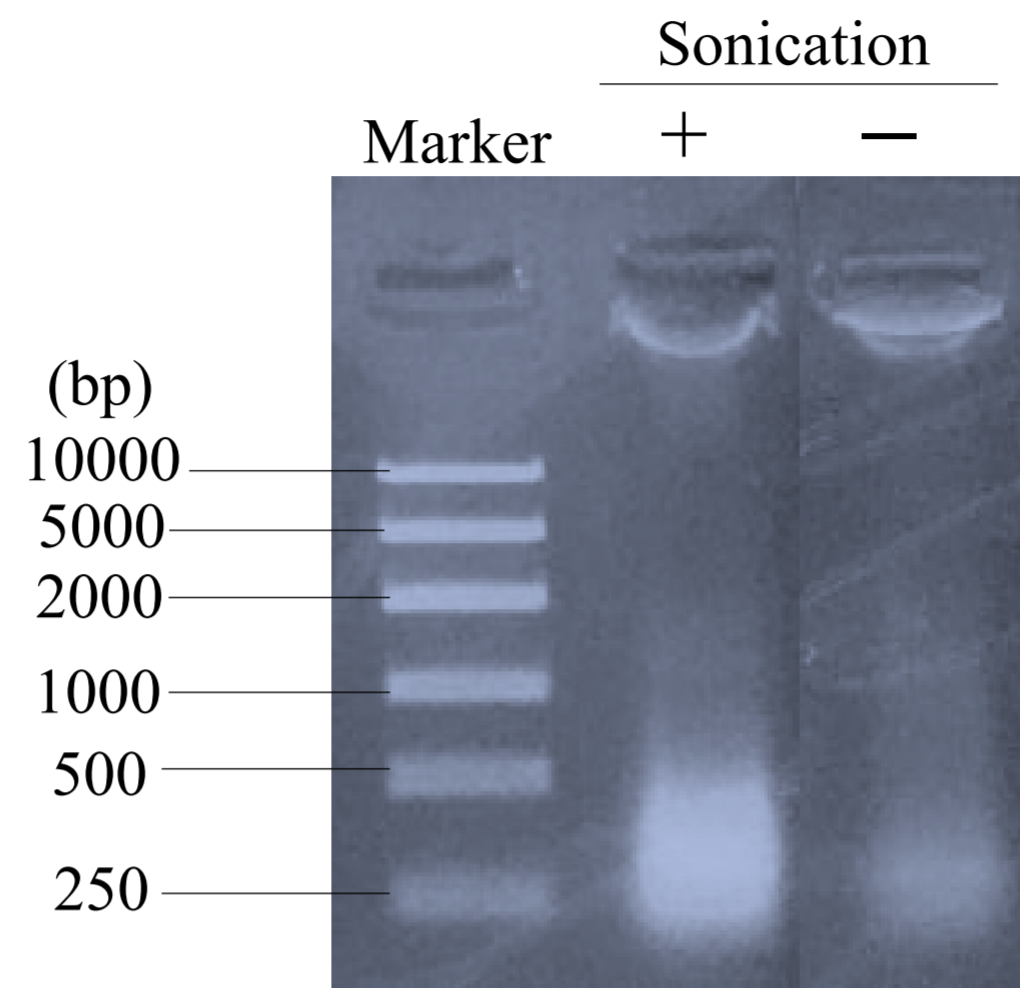


Fig.3

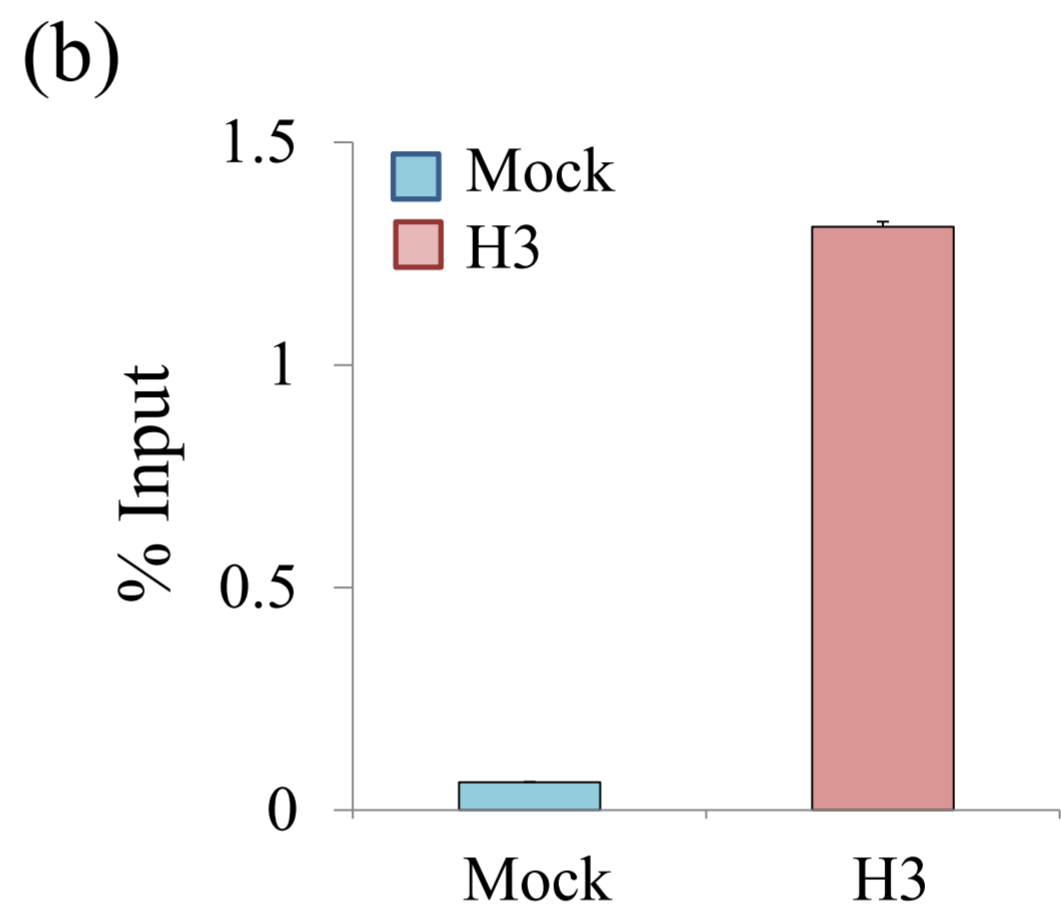
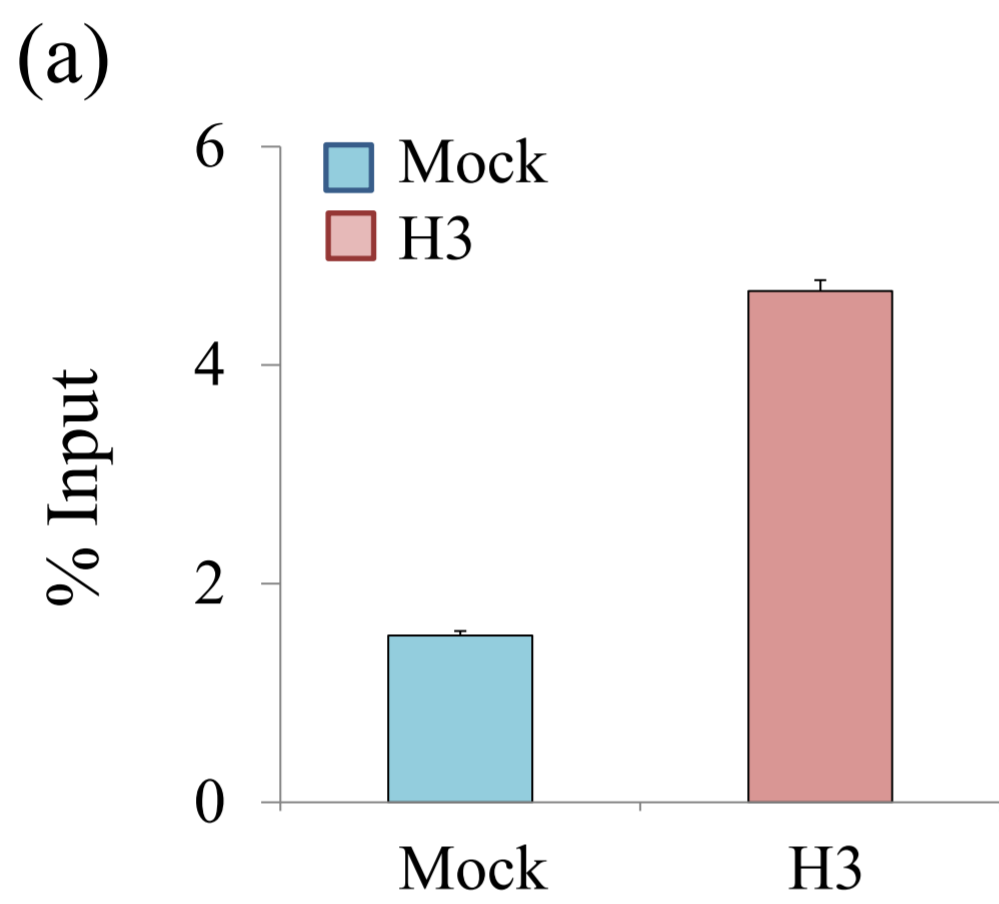


Fig.4

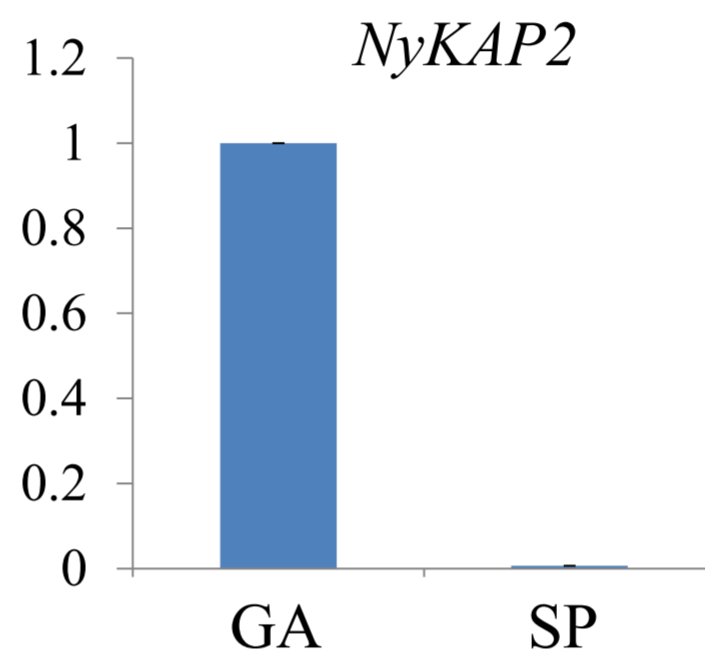
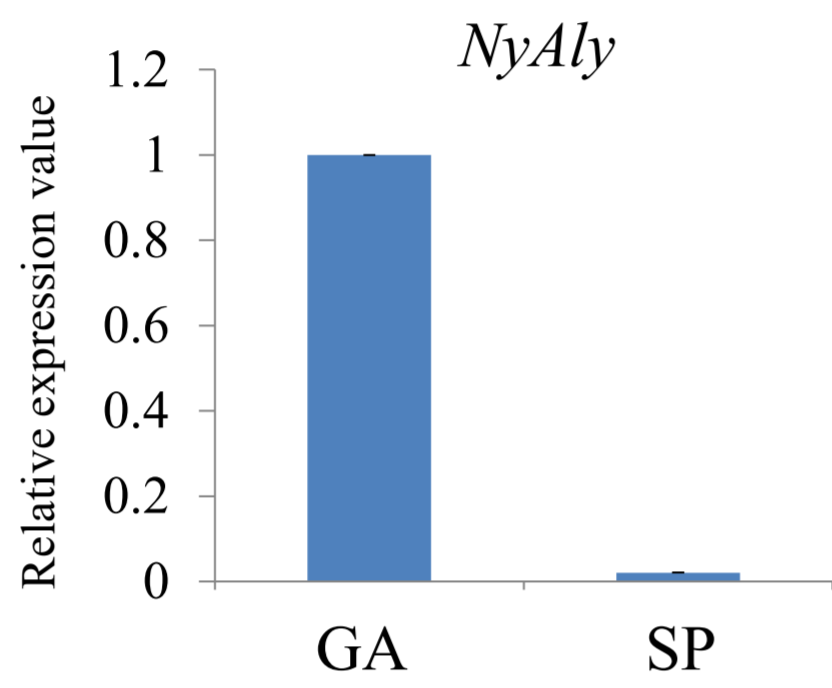
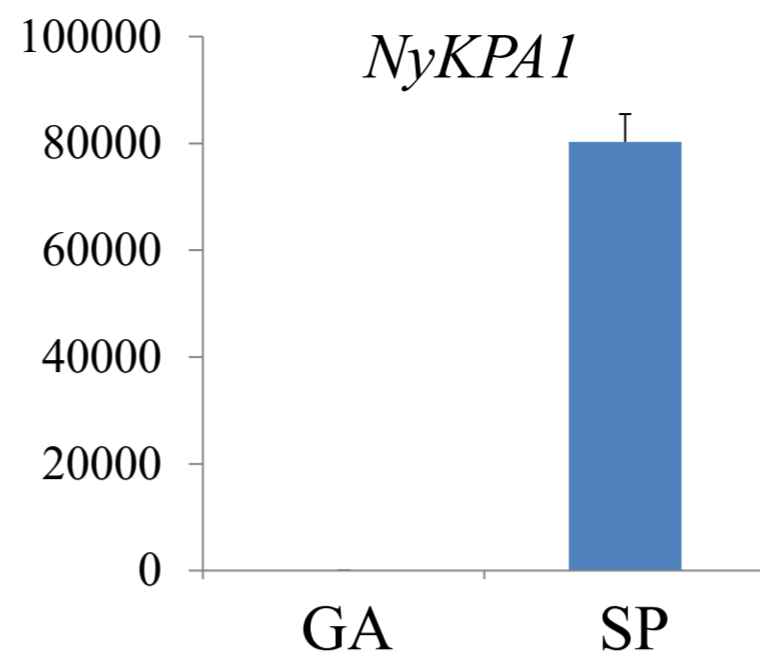
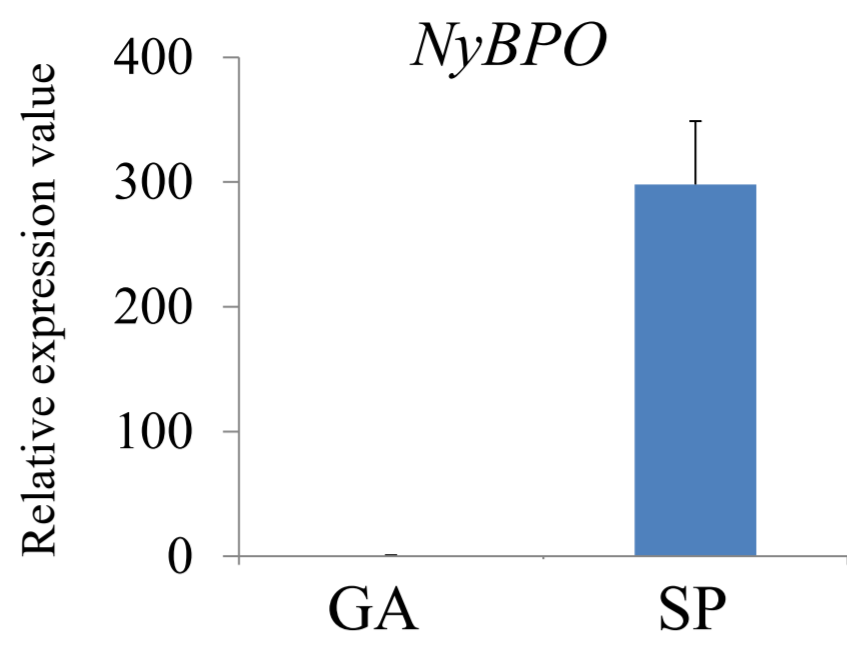


Fig.5

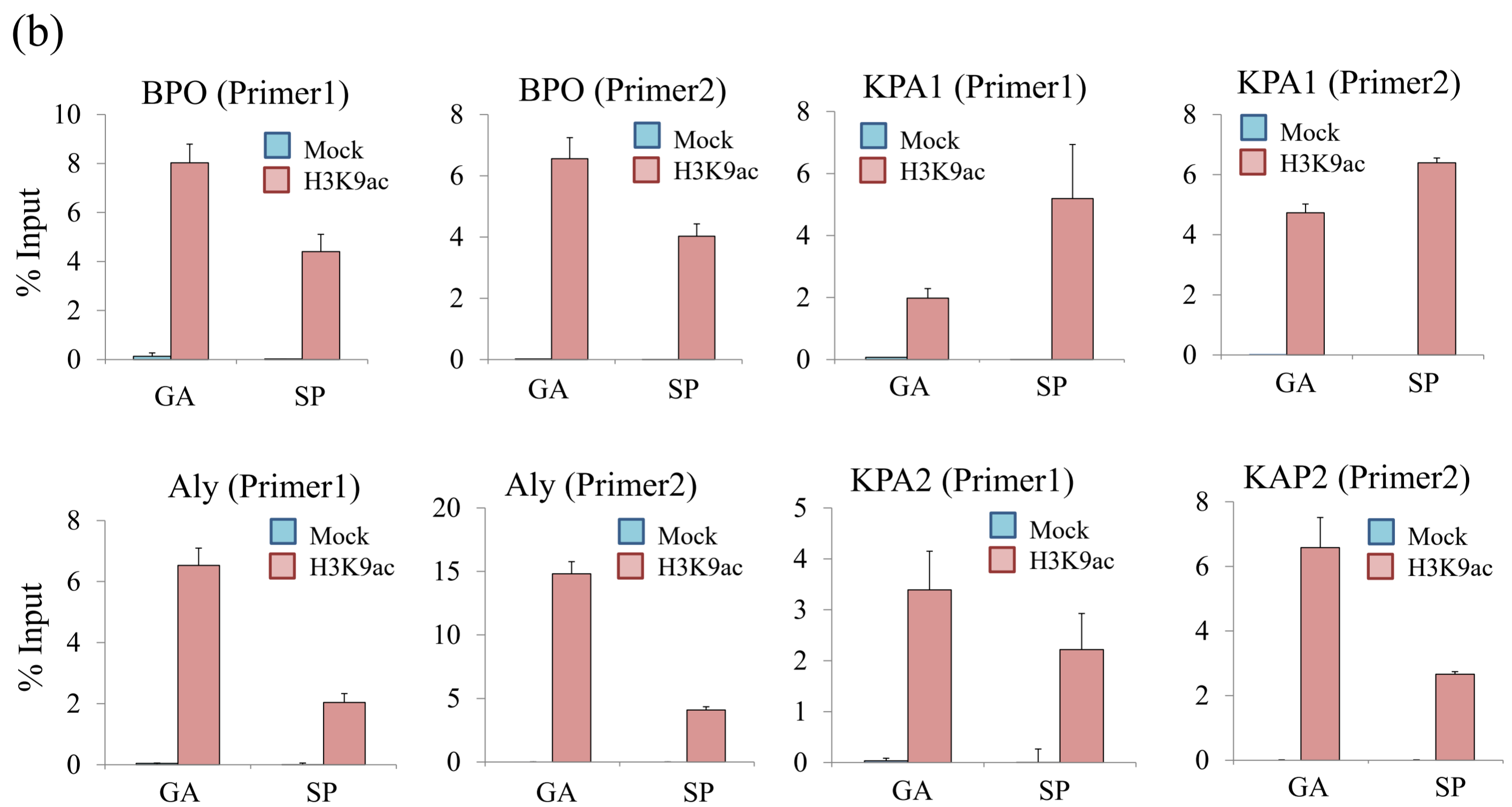
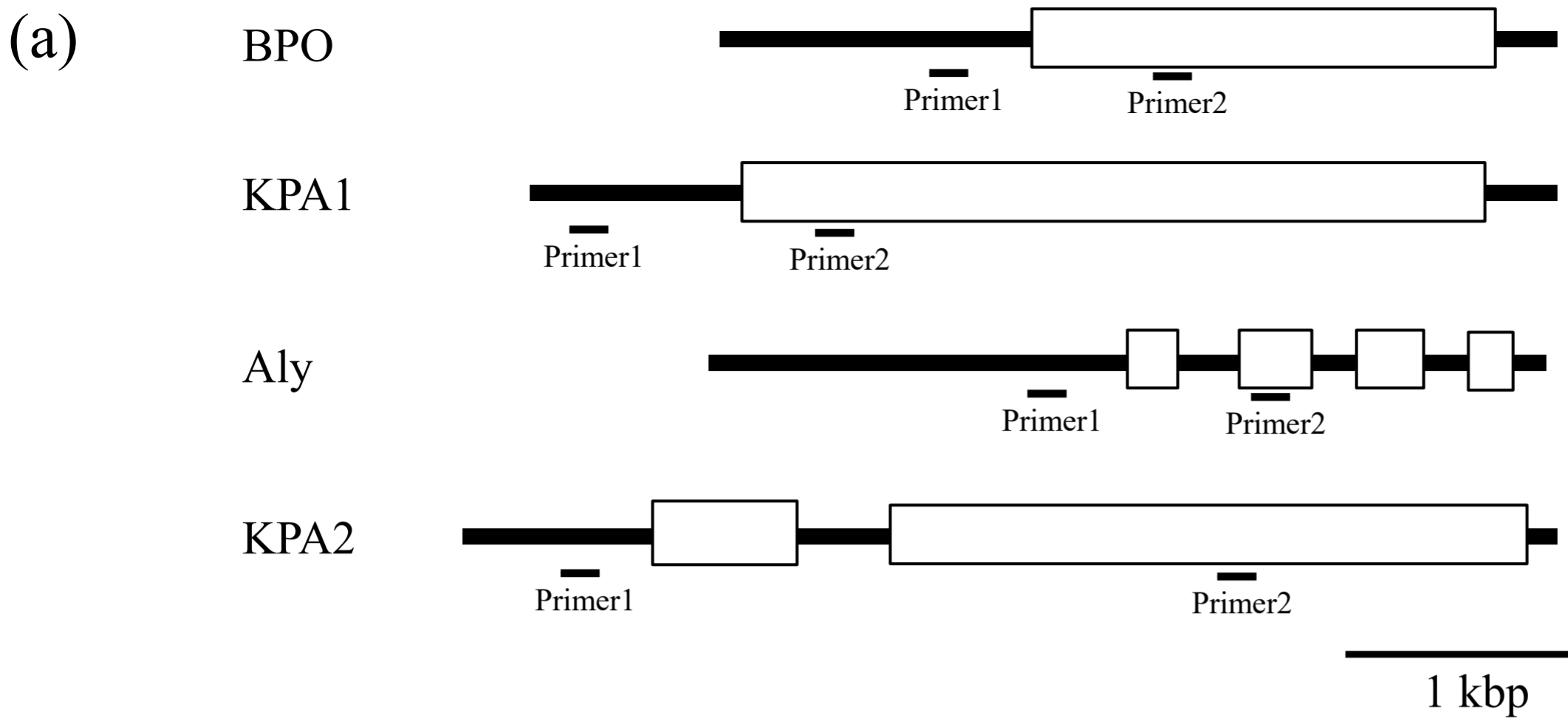


Fig.6